

# On the Thermal Behavior of the Slab in a Reheating Furnace with Radiation

Gyo Woo Lee, Man Young Kim

**Abstract**—A mathematical heat transfer model for the prediction of transient heating of the slab in a direct-fired walking beam type reheating furnace has been developed by considering the nongray thermal radiation with given furnace environments. The furnace is modeled as radiating nongray medium with carbon dioxide and water with five-zoned gas temperature and the furnace wall is considered as a constant temperature lower than furnace gas one. The slabs are moving with constant velocity depending on the residence time through the non-firing, charging, preheating, heating, and final soaking zones. Radiative heat flux obtained by considering the radiative heat exchange inside the furnace as well as convective one from the surrounding hot gases are introduced as boundary condition of the transient heat conduction within the slab. After validating thermal radiation model adopted in this work, thermal fields in both model and real reheating furnace are investigated in terms of radiative heat flux in the furnace and temperature inside the slab. The results show that the slab in the furnace can be more heated with higher slab emissivity and residence time.

**Keywords**—Reheating Furnace, Steel Slab, Radiative Heat Transfer, WSGGM, Emissivity, Residence Time.

## I. INTRODUCTION

THE reheating process has been commonly used to raise the slab temperature so that the subsequent hot-rolling process can run on wheels. The reheating process has two kinds of different objectives. The first one is to raise the slab temperature nearly up to 1,200°C and keep the temperature difference within the slab as small as possible (generally,  $\pm 5^\circ\text{C}$ ) around the target temperature in order to improve the steel quality [1]. The other one is related to the combustion, i.e., the reheating process should have lower energy consumption and combustion-generated pollutant emissions [2]-[5]. Therefore, combustion and heat transfer analysis in a reheating furnace is highly demanded.

It is well known that the slab in a furnace is heated by conductive, convective, and radiative heat transfer [6]. While the conductive and convective heat transfer occur due to the hot combustion gases, radiative heat transfer comes from both hot combustion gases and furnace walls. Among those three modes of heat transfer, the thermal radiation does play the most important role as its contribution to slab heating is above 90% of total heat flux from hot combustion gases and furnace walls in a reheating furnace. It is also well known that the furnace

wall is nearly black so that radiation from hot walls is only related to furnace temperature itself, while the hot combustion gases selectively heat the slab due to the spectral emission and absorption of  $\text{CO}_2$  and  $\text{H}_2\text{O}$  [7]-[11]. Therefore, nongray behavior of the combustion gases should be carefully considered in order to accurately model the furnace heat transfer.

In a few decades, numerous simulation models for furnace combustion and heat transfer for the prediction of the heating characteristics of a slab in a reheating furnace have been proposed. While Kim et al. [12] performed these three dimensional analysis with the turbulent reactive flow and radiative heat transfer in a walking beam type slab reheating furnace by using the commercial software FLUENT, and predicted the temperature distribution in the furnace and the heat fluxes on the upper and lower surfaces of slabs, Han et al. [13] conducted a similar analysis and estimated the thermal situations within a furnace including skid mark formation. Hsieh et al. [14] analyzed a three-dimensional turbulent combusting flow with the radiative heat transfer analysis in a walking beam types labre heating furnace with the commercial STAR-CD code. Chapman et al. [15] performed the parametric studies on effects of slab and refractory wall emissivities and the height of the combustion space on the thermal performance of a continuous reheating furnace. Meanwhile, Han et al. [16] divided an entire furnace into 14 homogeneous sub-zones and calculated medium temperature for all the sub-zones based on the overall heat balance. Jaklic et al. [17] investigated the influence of the space between billets on the productivity of a continuous walking-beam furnace with the Monte Carlo method for radiation and 3D finite-difference method for heat conduction in the billets. Also, Kim [1] developed a heat transfer model to analyze the transient heating of a slab in a direct-fired walking beam type reheating furnace by the finite volume method (FVM) for both conduction and radiation and examined the radiative characteristics in the furnace and the thermal behaviors of the slab with a medium temperature that was experimentally obtained. After that, Jang et al. [18], [19] investigated skid mark formations and slab heating phenomena according to the formation and growth of a scale on the slab surface. Recently, Lee and Kim [20] investigated the optimum residence time for steel productivity and energy saving in a three-zoned reheating furnace by comparing between the cold charge rolling (CCR) and hot charge rolling (HCR) conditions with two different furnace temperature and environments.

Based on the previous researches in this field, the overall heat transfer characteristics in a furnace are investigated in this work. After introducing the mathematical models for slab heat

Gyo Woo Lee, Associate Professor, is with the Department of Mechanical Design Engineering, Chonbuk National University, Jeonju, Chonbuk 561-756, Republic of Korea.

Man Young Kim, Corresponding Author, is with the Professor, Department of Aerospace Engineering, Chonbuk National University, Jeonju, Chonbuk 561-756, Republic of Korea (e-mail: manykim@jbnua.ac.kr).

conduction and radiative and conductive heat fluxes as a boundary condition, numerical approach to attack the radiative transfer equation (RTE) with nongray gas model named weighted sum of gray gases model (WSGGM) [7], [8] is introduced to get the radiative heat flux. To find the thermal development in the furnace, two different model furnaces are examined in terms of radiative heat flux and temperature of the inserts. After that, thermal development of the slab and radiative fields inside the furnace are investigated by changing parameters such as emissivity and residence time of the slab in the furnace. Finally, some concluding remarks are presented.

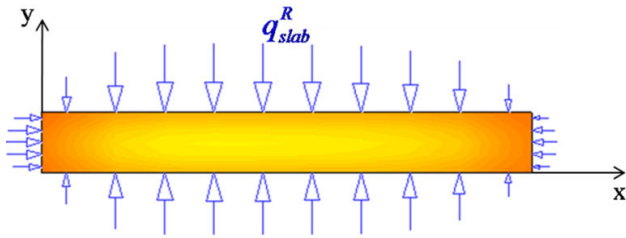


Fig. 1 Schematic of the total heat flux entering the slab surface

## II. MATHEMATICAL FORMULATION

### A. Governing Equations

The two dimensional transient heat conduction equation with a steel slab is given by

$$\rho C \frac{\partial T}{\partial t} = \frac{\partial}{\partial x} \left( k \frac{\partial T}{\partial x} \right) + \frac{\partial}{\partial y} \left( k \frac{\partial T}{\partial y} \right) \quad (1)$$

where,  $\rho$ ,  $C$  and  $k$  represent the density, specific heat, and conductivity of the slab, respectively. The total heat flux,  $q_{slab}^T = q_{slab}^C + q_{slab}^R$ , shown in Fig. 1, which can be obtained from the summation of the convective and radiative heat fluxes. Here, the convective heat flux,  $q_{slab}^C$  between the furnace gas and the solid slab surface is evaluated as

$$q_{slab}^C = h(T_g - T_{slab}) \quad (2)$$

where  $h$  is the gas convective heat transfer coefficient at the surface of the slab, equal to  $7.8 \text{ W/m}^2\text{K}$  [18]. The radiative heat flux,  $q_{slab}^R$  on the slab surface is calculated with the following equation,

$$q_{slab}^R = \int_{\Omega=4\pi} I(\vec{r}_{slab}, \vec{s})(\vec{s} \cdot \vec{n}_{slab}) d\Omega \quad (3)$$

where  $I(\vec{r}_{slab}, \vec{s})$  is the radiation intensity at the slab surface  $\vec{r}_{slab}$  and direction  $\vec{s}$ ,  $\vec{n}_{slab}$  is the outward unit normal vector at the slab surface, and  $\Omega$  is the solid angle. The radiative heat flux can be calculated after solving the radiative transfer equation (RTE) to get the radiative intensity on the slab,  $I(\vec{r}_{slab}, \vec{s})$ .

### B. Formulation of RTE with WSGGM

Combustion products such as  $\text{CO}_2$  and  $\text{H}_2\text{O}$  have highly spectral characteristics. The WSGGM [7], [8] is used to model the spectral behaviors of combustion products of  $\text{CO}_2$  and  $\text{H}_2\text{O}$  in the furnace. The governing WSGGM-based RTE can be expressed as

$$\frac{dI_k^m(\vec{r})}{ds} = -\kappa_{a,k} I_k^m(\vec{r}) + \kappa_{a,k} \omega_k I_b(\vec{r}) \quad (4)$$

where  $I_k^m(\vec{r})$  is the  $k$  th band radiative intensity at location  $\vec{r}$  and direction  $m$ . The  $\kappa_{a,k}$  and  $\omega_k$  denote  $k$  th gray band absorption coefficient and corresponding weighting factor, respectively. Meanwhile, for a diffusely emitting and reflecting furnace wall with temperature, the outgoing intensity can be expressed as the summation of the emitted and reflected ones such as,

$$I_k^m(\vec{r}_w) = \varepsilon_w \omega_k I_{bw}(\vec{r}_w) + \frac{1 - \varepsilon_w}{\pi} \int_{\vec{s}' \cdot \vec{n}_w < 0} I_k^{m'}(\vec{r}_w) |\vec{s}' \cdot \vec{n}_w| d\Omega' \quad (5)$$

where  $\varepsilon_w$  is the wall emissivity and  $I_{bw}(\vec{r}_w)$  is the blackbody intensity of the surrounding wall. Finally, the radiative heat flux in (3) estimated from the total intensity as,

$$q_{slab}^R = \sum_{k=1}^K q_{slab,k}^R = \sum_{k=1}^K \int_{\Omega=4\pi} I_k^m(\vec{r}_{slab})(\vec{s} \cdot \vec{n}_{slab}) d\Omega \quad (6)$$

In the conventional WSGGM [7] adopted in this work, four gray gases are commonly used ( $K = 4$ ) with spectral window of  $\kappa_{a,k} = 0$  when  $K = 1$ . Here, it is noted that total ( $m \times k$ ) RTEs have to be solved at each location and direction to find the whole intensity fields and corresponding radiative heat fluxes.

### C. Solution Procedure

The transient heat conduction equation in (1) is discretized by using the conventional finite volume approach [21]. A central differencing scheme is used for the diffusion terms, while the unsteady term is treated implicitly. The resulting discretized system is then solved iteratively by using the TDMA (tridizgonal matrix algorithm) algorithm until the temperature field in the slab satisfies the following convergence criterion:

$$\max \left( \left| T_{i,j}^n - T_{i,j}^{n-1} \right| / T_{i,j}^n \right) \leq 10^{-6} \quad (7)$$

where  $T_{i,j}^{n-1}$  is the previous value of  $T_{i,j}^n$  in the same time level.

In order to compute the radiative heat flux on the slab surface in (6), which is one of the boundary conditions of (1), the RTE, (4) must be accurately analyzed. In this work, the FVM for radiation is employed to attack the RTE. Detailed information on FVM for radiation can be found in Chui and Raithby [22],

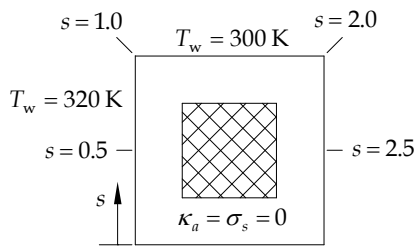
and developed by Chai et al. [23], and Baek et al. [24].

III. RESULTS AND DISCUSSION

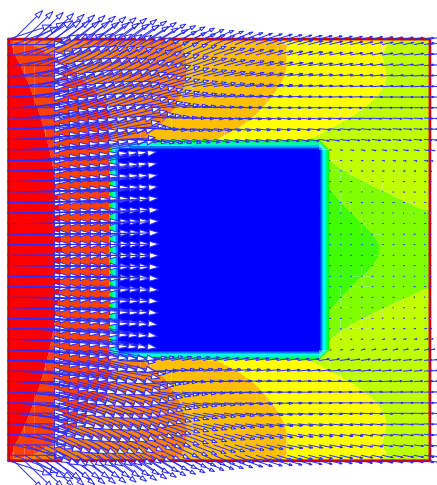
A. Code Validation

For the first example, radiation in a square enclosure with a central block is investigated. The schematics are shown in Fig. 2 (a). The enclosure wall at west face is hot at 320 K, while all other walls and a central blockage of 0.5m×0.5m are maintained at 300 K. All walls including a central blockage are assumed black. The enclosed medium is transparent, i.e.,  $\kappa_a = 0$  with no scattering. The spatial and angular grid systems used are  $N_x = 40$ ,  $N_y = 40$ ,  $N_\theta = 4$ , and  $N_\phi = 40$ , respectively.

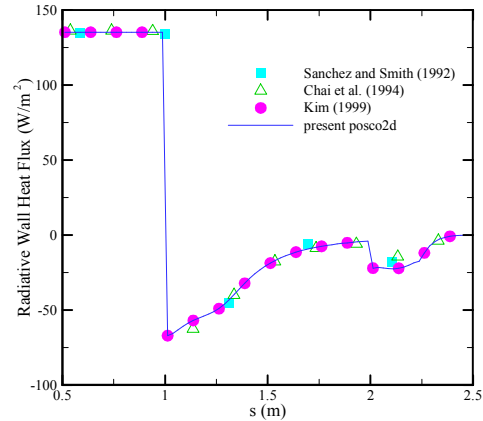
Fig. 2 (b) shows the radiative heat flux vectors with incident radiation contours in the background. As expected, all of the radiative heat comes from the hot west wall, and the central blockage blocks the radiative heat, therefore, it can be observed that there is little radiative heat flux in the east region of the central blockage. The predicted wall heat flux along the enclosure walls is depicted in Fig. 2 (c). The present solutions are compared with other solutions obtained by the RIM [25] and blocked-off FVM [26]. It can be found that the present solutions well capture the other ones, especially discontinuity at  $s = 1\text{ m}$ , and the uniform heat flux of  $135.27\text{ W/m}^2$ , which equals to exact heat flux of  $\sigma(T_h^4 - T_c^4) = 135.27\text{ W/m}^2$  on the west wall ( $0.5 \leq s \leq 1\text{ m}$ ).



(a) Schematic of the problem



(b) Radiative heat flux vectors with incident radiation

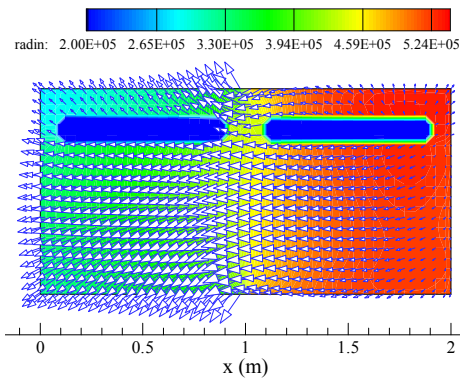


(c) Radiative heat flux on the surface

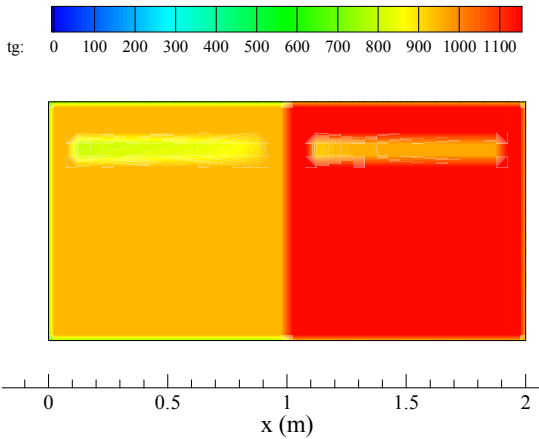
Fig. 2 A square enclosure with a central blockage. All walls and a central blockage are black. The west wall is hot as 320 K, while all other walls and a central blockage are cold as 300K

B. Slabs in a Model Furnace

The reheating furnace heat transfer model with nongray thermal radiation is applied to investigate thermal behaviors of the furnace and slab such as radiative heat flux in the furnace and temperature distribution within the slab. Firstly, the model furnace which resembles the real furnace is considered to examine the thermal development of the slab. In Fig. 3, two slabs with length of 0.8m and width of 0.1m are located at the height of 0.8m in the furnace with 2m×1m. All the surface has emissivity of 1.0. The temperature of the slab can vary with time, while the furnace is filled with hot gases, 950 °C in the left half and 1,150 °C in the right half sections, respectively. The wall temperatures are 200 °C lower than enclosed gases. Fig. 3 shows the radiative heat flux vectors with incident radiation in the background and temperature of the slab in steady-state. In this figure, it can be found that the radiative heat flux is towards the cold wall and strongly enters the wall where temperature discontinuity exists. The surface temperature is seen to be heated nearly up to the temperature of surrounding gases. Also, the right side of each slab is more heated because of the furnace temperature conditions adopted in this model.



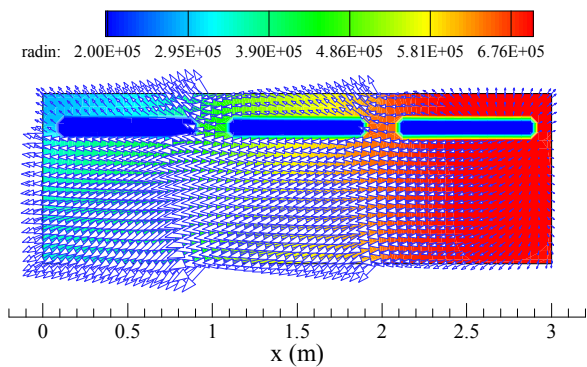
(a) Radiative heat flux vectors with incident radiation



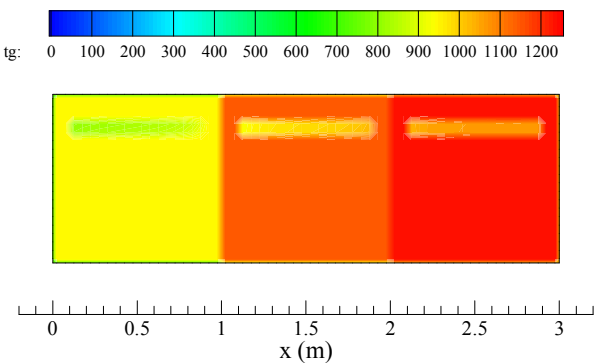
(b) Temperature distribution in furnace and slab

Fig. 3 Thermal fields of radiative heat flux vectors and temperature within the furnace with two slabs in a model furnace of 2m x 1m

Fig. 4 is the case for three slabs in the model furnace of 3m x 1m. All the conditions and properties are same in case of two slabs except the medium temperatures are 950 °C, 1,150 °C, and 1,240 °C from left zone, respectively. It also can be observed the same thermal behaviors of the slab and furnace.



(a) Radiative heat flux vectors with incident radiation



(b) Temperature distribution in furnace and slab

Fig. 4 Thermal fields of radiative heat flux vectors and temperature within the furnace with three slabs in a model furnace of 3m x 1m

C. Slabs in a Real Furnace

The present numerical model is applied to a real furnace shown in Fig. 5. The furnace consists of five zones, i.e., non-firing where slabs are pushed into the furnace, charging, preheating, heating, and final soaking zones. The temperature of the furnace wall and gases used for the simulation are listed in Table I, and the thermophysical properties of the slab are given in Table II, respectively. The furnace gases are composed of 7.6% CO<sub>2</sub>, 4.5% H<sub>2</sub>O, and remaining N<sub>2</sub> gases, while it is assumed that there are no particles, hence, no scattering.

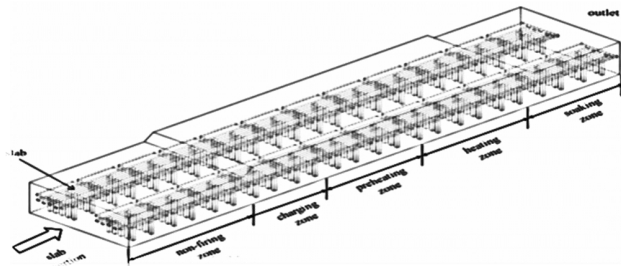


Fig. 5 Schematic of the real reheating furnace

TABLE I  
TEMPERATURE CONDITIONS OF FURNACE GASES AND THE WALL

zone	$T_{w\_upper}$	$T_{g\_upper}$	$T_{g\_lower}$	$T_{w\_lower}$
Non-firing	700	800	750	650
charging	843	943	890	790
preheating	1,014	1,114	1,060	960
heating	1,073	1,173	1,171	1,071
soaking	1,083	1,183	1,170	1,070

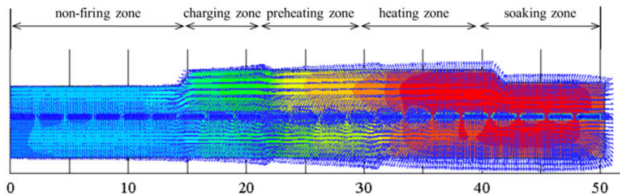
TABLE II  
THERMAL PROPERTIES OF THE SLAB

Temp. (°C)	Conductivity (W/mK)	Specific Heat (J/kgK)	Density (kg/m <sup>3</sup> )
30	26.89	299.0	
400	25.44	401.6	
600	22.70	512.0	7778
800	20.89	542.8	
1,000	23.69	478.9	

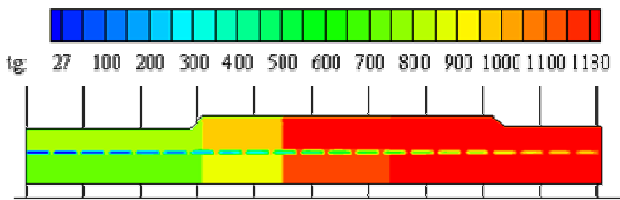
Fig. 6 (a) shows the radiation behavior in the furnace chamber, i.e., radiative heat flux vectors and incident radiation in the background. Note that in the first two zones radiative heat flux vectors are concentrated on the slab located at the near center of the furnace height, which means that high amounts of heating is made in these early zones of the furnace. Steel slabs are more heated by passing through the adjacent preheating and heating zones, thereby, peak temperature appears in the heating zone. On the other hand, in the final soaking zone, because the furnace temperature is slightly down than the previous heating zone and the slab is in high temperature nearly to the furnace gas temperature, some radiative heat flux is emitted from the hot slab, which is the reverse phenomenon compared with the situation in the previous zones. Therefore, temperature of the slab is slightly lowered and the temperature gradient within the slab becomes smaller. Fig. 6 (b) illustrates the temperature distribution of the total 22 slabs with the five zone furnace. The



first slab charged into the non-firing zone with 25 °C receives strong thermal radiation from hot furnace gases and wall because of relatively high temperature difference between the slab and others. As is expected, the slabs are more heated up as passing through the subsequent charging, preheating, and heating zones nearly to 1,180 °C. Temperature within the slab, however, is slightly lowered and somewhat equilibrated in the final soaking zone for the subsequent rolling process.



(a) Radiative heat flux vectors with incident radiation



(b) Temperature distribution in furnace and slab

Fig. 6 Thermal fields of radiative heat flux vectors and temperature within the real furnace.

The effect of slab emissivity on the slab temperature is shown in Fig. 7. It can be seen that the temperature of the slab increases with the slab emissivity because the slab can receive more radiant heat from surrounding hot gases and furnace wall. Fig. 8 depicts the effect of residence time on the slab temperature. As expected, as the residence time becomes longer, which means slabs can stay more in the furnace, more heat is transferred to the slab, which leads to higher slab temperature.

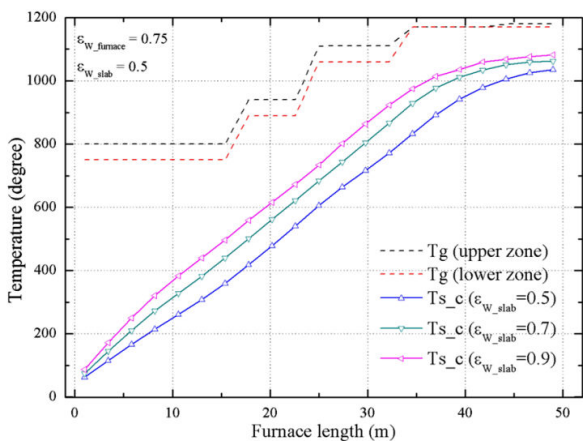


Fig. 7 Effect of slab wall emissivity on the predicted longitudinal slab temperature

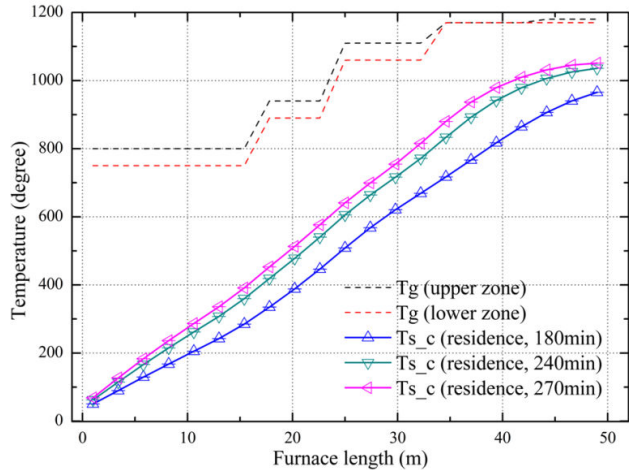


Fig. 8 Effect of residence time on the predicted longitudinal slab temperature

IV. CONCLUSION

In this work a mathematical model for a furnace heat transfer with nongray gas radiation has been examined and applied to the model and real furnaces. After validating the present numerical results with other solutions, effects of slab emissivity and residence time on heat transfer are investigated in view of development of the slab temperature. The results show that the slab inside the furnace is more heated with higher emissivity and residence time.

ACKNOWLEDGMENT

This work was supported by Basic Science Research Program through the National Research Foundation of Korea (NRF) funded by the Ministry of Education, Science and Technology (grant number 2011-0022179). Also, this research was partially supported by Leading Foreign Research Institute Recruitment Program through the National Research Foundation of Korea funded by the Ministry of Education, Science and Technology (2011-0030065).

REFERENCES

- [1] M. Y. Kim, "A heat transfer model for the analysis of transient heating of the slab in a direct-fired walking beam type reheating furnace," *International Journal of Heat and Mass Transfer*, vol. 50, 2007, pp. 3740-3748.
- [2] D. Wild, T. Meurer, and A.Kugi, "Modelling and experimental model validation for a pusher-type reheating furnace," *Mathematical and Computer Modelling of Dynamical Systems*, vol.15, 2009, pp. 209-232.
- [3] C.-T. Hsieh, M.-J. Huang, S.-T. Lee, and C.-H. Wang, "A numerical study of skid marks on the slabs in a walking-beam type slab reheating furnace," *Numerical Heat Transfer, Part A*, vol. 57, 2010, pp. 1-17.
- [4] V. Panjkovic and R. Gloss, "Fast dynamic heat and mass balance model of walking beam reheat furnace with two-dimensional slab temperature profile," *Ironmaking& Steelmaking*, vol. 39, 2012, pp. 190-209.
- [5] A. Emadi, A. Saboonchi, M. Their, and S. Hassanpour, "Heating characteristics of billet in a walking hearth type reheating furnace," *Applied Thermal Engineering*, vol. 63, 2014, pp. 396-405.
- [6] S. H. Han, S. W. Baek, S. H. Kang, and C. Y. Kim, "Numerical analysis of heating characteristics of a slab in a bench scale reheating furnace," *International Journal of Heat and Mass Transfer*, vol. 50, 2007, pp. 2019-2023.

- [7] T. F. Smith, Z. F. Shen, and J. N. Friedman, "Evaluation of coefficients for the weighted sum of gray gases model," *Journal of Heat Transfer*, vol. 104, 1982, pp. 602-608.
- [8] M. F. Modest, "The weighted-sum-of-gray-gases model for arbitrary solution methods in radiative transfer," *Journal of Heat Transfer*, vol. 113, 1991, pp. 650-656.
- [9] T. K. Kim, J. A. Menart, and H. S. Lee, "Nongrayradiative gas analyses using the S-N discrete ordinates method," *Journal of Heat Transfer*, vol. 113, 1991, pp. 946-952.
- [10] T. H. Song, "Comparison of engineering models of nongray behavior of combustion products," *International Journal of Heat and Mass Transfer*, vol. 36, 1993, pp. 3975-3982.
- [11] M. K. Denison and B. W. Webb, "A spectral line-based weighted-sum-of-gray-gases model for arbitrary RTE solvers," *Journal of Heat Transfer*, vol. 115, 1993, pp. 1004-1012.
- [12] J. G. Kim, K. Y. Huh, and I. T. Kim, "Three-dimensional analysis of the walking-beam-type slab reheating furnace in hot strip mills," *Numerical Heat Transfer, Part A*, vol. 38, 2000, pp. 589-609.
- [13] S. H. Han, D. Chang, and C. Y. Kim, "A numerical analysis of slab heating characteristics in a walking beam type reheating furnace," *International Journal of Heat and Mass Transfer*, vol. 53, 2010, pp. 3855-3861.
- [14] C.-T. Hsieh, M.-J. Huang, S.-T. Lee, and C.-H. Wang, "Numerical modeling of a walking-beam-type slab reheating furnace," *Numerical Heat Transfer, Part A*, vol. 53, 2008, pp. 966-981.
- [15] K. S. Chapman, S. Ramadhyani, and R. Viskanta, "Modeling and parametric studies of heat transfer in a direct-fired continuous reheating furnace," *Metallurgical Transactions*, vol. 22B, 1991, pp. 513-521.
- [16] S. H. Han, D. Chang, and C. Huh, "Efficiency analysis of radiative slab heating in a walking-beam-type reheating furnace," *Energy*, vol. 36, 2011, pp. 1265-1272.
- [17] A. Jaklic, T. Kolenko, and B. Zupancic, "The influence of the space between the billets on the productivity of a continuous walking-beam furnace," *Applied Thermal Engineering*, vol. 25, 2005, pp. 783-795.
- [18] J. H. Jang, D. E. Lee, C. Kim, and M. Y. Kim, "Prediction of furnace heat transfer and its influence on the steel slab heating and skid mark formation in a reheating furnace," *ISIJ International*, vol. 48, 2008, pp. 1325-1330.
- [19] J. H. Jang, D. E. Lee, M. Y. Kim, and H. G. Kim, "Investigation of the slab heating characteristics in a reheating furnace with the formation and growth of scale on the slab surface," *International Journal of Heat and Mass Transfer*, vol. 53, 2010, pp. 4326-4332.
- [20] D. E. Lee and M. Y. Kim, "Optimum residence time for steel productivity and energy saving in a hot rolled reheating furnace," *Journal of Mechanical Science and Technology*, vol. 27, 2013, pp. 2869-2877.
- [21] S. V. Patankar, *Numerical Heat Transfer and Fluid Flow*, Mc-Graw Hill, New York, 1980.
- [22] E. H. Chui and R. D. Raithby, "Computation of radiant heat transfer on a nonorthogonal mesh using the finite-volume method," *Numerical Heat Transfer, Part B*, vol. 23, 1993, pp. 269-288.
- [23] J. C. Chai, H. S. Lee, and S. V. Patankar, "Finite-volume method for radiation heat transfer," *Journal of Thermophysics and Heat Transfer*, vol. 8, 1994, pp. 419-425.
- [24] S. W. Baek, M. Y. Kim, and J. S. Kim, "Nonorthogonal finite-volume solutions of radiative heat transfer in a three-dimensional enclosure," *Numerical Heat Transfer, Part B*, vol. 34, 1998, pp. 419-437.
- [25] A. Sanchez and T. F. Smith, "Surface radiation exchange for two-dimensional rectangular enclosure using the discrete ordinates method," *Journal of Heat Transfer*, vol. 114, pp. 415-417.
- [26] J. C. Chai, H. S. Lee, and S. V. Patankar, "Treatment of irregular geometries using a Cartesian coordinates finite-volume radiation heat transfer procedure," *Numerical Heat Transfer, Part B*, vol. 26, 1994, pp. 225-235.